How Long Is Long Enough When Measuring Fluxes and Other Turbulence Statistics?

D. H. LENSCHOW, J. MANN,* AND L. KRISTENSEN*

National Center for Atmospheric Research,† Boulder, Colorado

(Manuscript received 2 November 1992, in final form 16 August 1993)

ABSTRACT

It is determined how long a time series must be to estimate covariances and moments up to fourth order with a specified statistical significance. For a given averaging time T there is a systematic difference between the true flux or moment and the ensemble average of the time means of the same quantities. This difference, referred to here as the systematic error, is a decreasing function of T tending to zero for $T \to \infty$. The variance of the time mean of the flux or moment, the so-called error variance, represents the random scatter of individual realizations, which, when T is much larger than the integral time scale $\mathcal{T}$ of the time series, is also a decreasing function of T. This makes it possible to assess the minimum value of T necessary to obtain systematic and random errors smaller than specified values. Assuming that the time series are either Gaussian processes with exponential correlation functions or a skewed process derived from a Gaussian, we obtain expressions for the systematic and random errors. These expressions show that the systematic error and the error variance in the limit of large T are both inversely proportional to T, which means that the random error, that is, the square root of the error variance, will in this limit be larger than the systematic error. It is demonstrated theoretically, as well as experimentally with aircraft data from the convective boundary layer over the ocean and over land, that the assumption that the time series are Gaussian leads to underestimation of the random errors, while derived processes with a more realistic skewness and kurtosis give better estimates. For fluxes, the systematic and random errors are estimated when the time series are sampled instantaneously, but the samples separated in time by an amount Δ. It is found that the random error variance and the systematic error increase by less than 8% over continuously sampled data if Δ is no larger than the integral scale obtained from the flux time series and the cospectrum, respectively.

1. Introduction

A fundamental tool in studying turbulence processes is the use of statistical moments to describe the properties of a field of turbulent fluctuations. Ideally the statistical moments should be determined by ensemble averaging, but in practical experimental situations this is not possible. Instead, the moments are estimated by a finite number of sample averages over a finite time period. Since theoretical treatments of turbulence often assume ensemble-averaged statistical moments, it is an important practical consideration to be able to estimate the difference between measured moments and the idealized ensemble-averaged moments that they are assumed to represent.

Recent observational studies such as the First ISLSCP (International Satellite Land Surface Climatology Project) Field Experiment (FIFE) and the Atmospheric Boundary Layer Experiments (ABLE) have renewed interest in examining the significance of turbulence statistics measurements. This interest is related to such issues as the effects of changes in greenhouse gas concentrations on climate and on understanding the interaction of vegetated land surfaces with the atmosphere (Lenschow and Hicks 1989). One example of the importance of this issue is the observation by Betts et al. (1990), Kelly et al. (1992), and Grossman (1992) of a significant reduction in airplane-measured scalar fluxes in FIFE due to inadequate length of flight legs and high-pass filtering.

Another example is the comparison of large-eddy simulation (LES) and direct simulation results with observations. For example, measurements of third-order moments do not always agree with LES, and in some cases it is not clear whether the differences are statistically significant. Moeng and Rotunno (1990), for example, have carried out direct simulations of buoyancy-driven turbulence and found that their simulations differ significantly from observations in a convective boundary layer. Similarly, large-eddy simulations of the convective atmospheric boundary layer (Schmidt and Schumann 1989; Mason 1989) make predictions about the behavior of turbulence statistics, and again differences between simulated and observed

* Permanent affiliation: Risø National Laboratory, Roskilde, Denmark.

† The National Center for Atmospheric Research is sponsored by the National Science Foundation.

Corresponding author address: Dr. Donald H. Lenschow, NCAR, P.O. Box 3000, Boulder, CO 80307-3000.

© 1994 American Meteorological Society

Unauthenticated | Downloaded 02/15/25 07:08 AM UTC

values, particularly for third moments, are found. However, observations of the third-order moment contain considerable scatter and are difficult to measure accurately. LeMone (1990) discusses some observations of skewness and possible sources of error in skewness measurements. Her approach is to investigate the effects of specific mesoscale phenomena in altering skewness rather than a general approach for estimating the significance of measurements of higher-order moments.

For these reasons, we have carried out a detailed evaluation of the error generated in second-, third-, and fourth-order moments of a single variable, and in covariances of two variables (e.g., fluxes) due to using measured time series of limited length to estimate the ensemble statistics. This error contains both a systematic and a random contribution. We also consider the additional error introduced by selecting an equally spaced subset of the original time series from which the covariance is computed. Practical applications of this include 1) use of sampling technology to grab an instantaneous sample of air whose constituents can then be measured in a more leisurely fashion with slower-responding sensors than required for direct measurements of the covariance without compromising the frequency response of the measurement, and 2) it may be possible to reduce the amount of data to be stored without increasing the error in the covariance estimates. We then compare the theoretical expressions with errors calculated from airplane measurements of vertical air velocity and temperature.

In the following analysis we consider only stationary time series. This implies that they must be of infinite duration. Real time series are, of course, never strictly stationary and very often they are far from it. For example, they often have significant trends, and often random fluctuations have a different character at different regions in the time series. We often then assume that the given time series is a part of an infinitely long stationary time series but that the given time series is too short for all these large-scale features to be statistically resolved. For this reason, real time series are often preprocessed to eliminate or suppress these large-scale features. Examples of preprocessing are *trend removal, time-dependent scaling or "windowing"* and high-pass filtering. Dealing with this inevitability of the real world requires skill, experience, and some a priori knowledge of the phenomenon under investigation to preprocess time series in such a way that the physical information is minimally corrupted.

The problem of estimating the statistical errors of higher moments has been addressed before by Lumley and Panofsky (1964). Their results have been discussed and applied by, for example, Wyngaard (1973) and Sreenivasan et al. (1978). As we discuss here, their approach differs from ours in that they do not separate systematic errors from random errors. It is quite natural to make this separation because averaged moments of second- and higher-order are functions of the averaging time (or length) and therefore systematically different from the theoretical ensemble values, which we can imagine to be the result of infinite averaging time. Furthermore, they predict only errors of second- and fourth-order moments, not third.

2. Systematic errors

In the following we separate the analysis into moments of one variable and moments of more than one variable. In the first category we deal with second, third, and fourth moments, whereas in the second we discuss only second moments, that is, covariances or fluxes.

a. Single time series moments

We consider an ergodic and consequently stationary time series $w(t)$ with the ensemble mean removed for notational convenience; that is,

$$\langle w(t)\rangle = 0. \tag{1}$$

The ensemble mean is, in experimental situations, estimated by the time average

$$w_T = \frac{1}{T}\int_{-T/2}^{T/2} w(t)dt, \tag{2}$$

which in general is different from $\langle w(t)\rangle$. However, taking the ensemble average of (2) implies

$$\langle w_T\rangle = \langle w(t)\rangle = 0. \tag{3}$$

By the assumption of ergodicity,

$$\lim_{T\to\infty}(w_T) = \langle w(t)\rangle. \tag{4}$$

The nth-order central moment is

$$\mu_n = \langle (w - \langle w\rangle)^n\rangle = \langle w^n\rangle, \tag{5}$$

which, in analogy to (2), is determined experimentally by time averaging; namely,

$$\mu_n(T) = \frac{1}{T}\int_{-T/2}^{T/2} [w(t) - w_T]^n dt. \tag{6}$$

In general, when $n > 1$,

$$\langle \mu_n(T)\rangle \neq \mu_n.$$

For the second-order moment we get

$$\langle \mu_2(T)\rangle = \frac{1}{T}\int_{-T/2}^{T/2}\langle [w(t) - w_T]^2\rangle dt$$

$$= \mu_2 - \frac{1}{T^2}\int_{-T/2}^{T/2} dt_1 \int_{-T/2}^{T/2} dt_2 \langle w(t_1)w(t_2)\rangle. \tag{7}$$

Since there will subsequently be several definite, multidimensional integrals of the type occurring in (7),

Unauthenticated | Downloaded 02/15/25 07:08 AM UTC

we introduce the short-hand notation of the n-dimensional, dimensionless integral operator:

$$\int \equiv \frac{1}{T^n}\int_{-T/2}^{T/2} dt_1 \int_{-T/2}^{T/2} dt_2 \cdots \int_{-T/2}^{T/2} dt_n. \quad (8)$$

Using this new convention, we get for the third- and fourth-order moments

$$\langle \mu_3(T)\rangle = \mu_3 - 3\int \langle w^2(t_1)w(t_2)\rangle + 2\int \langle w(t_1)w(t_2)w(t_3)\rangle \quad (9)$$

and

$$\langle \mu_4(T)\rangle = \mu_4 - 4\int \langle w^3(t_1)w(t_2)\rangle + 6\int \langle w^2(t_1)w(t_2)w(t_3)\rangle - 3\int \langle w(t_1)w(t_2)w(t_3)w(t_4)\rangle. \quad (10)$$

We define the autocovariance function $R_{ww}(\tau)$ and the autocorrelation function $\rho(\tau)$ by

$$R_{ww}(t_2 - t_1) = \langle w(t_1)w(t_2)\rangle \quad (11)$$

and

$$\mu_2\rho(t_2 - t_1) = R_{ww}(t_2 - t_1), \quad (12)$$

which, due to ergodicity and consequently, stationarity, are even functions of only one variable, namely, the time lag $\tau = t_2 - t_1$. From this it follows that the double integral in (7) can be reduced to a single integral,

$$\frac{\langle \mu_2(T)\rangle}{\mu_2} = 1 - \frac{2}{T}\int_0^T \left(1 - \frac{\tau}{T}\right)\rho(\tau)d\tau, \quad (13)$$

and in the limit $T \gg \mathcal{T}$,

$$\frac{\langle \mu_2(T)\rangle}{\mu_2} \approx 1 - 2\frac{\mathcal{T}}{T}, \quad (14)$$

where

$$\mathcal{T} = \int_0^\infty \rho(t)dt \quad (15)$$

is the integral time scale.

To estimate $\langle \mu_3(T)\rangle$ and $\langle \mu_4(T)\rangle$, we use the approximation that the signal can be derived from a Gaussian process. In the case of $\langle \mu_4(T)\rangle$, we assume that the signal itself is a Gaussian process. This implies that the Isserlis relation (Koopmans 1974)[1]

$$\langle w(t_1)w(t_2)w(t_3)w(t_4)\rangle = \langle w(t_1)w(t_2)\rangle\langle w(t_3)w(t_4)\rangle + \langle w(t_1)w(t_3)\rangle\langle w(t_2)w(t_4)\rangle + \langle w(t_1)w(t_4)\rangle\langle w(t_2)w(t_3)\rangle \quad (16)$$

can be applied to (10) to obtain in the limit $T \gg \mathcal{T}$

$$\frac{\langle \mu_4(T)\rangle}{\mu_4} \approx 1 - 4\frac{\mathcal{T}}{T}. \quad (17)$$

Lenschow et al. (1993, hereafter LMK) present the exact evaluation of (7) or (13) together with the fourth-order systematic error for all values of T assuming an exponential autocorrelation function

$$\rho(\tau) = \exp\left(-\frac{|\tau|}{\mathcal{T}}\right). \quad (18)$$

When evaluating (9), we obtain the trivial result that $\langle \mu_3(T)\rangle$, as well as all other odd moments, are zero if we assume that $w(t)$ is a Gaussian process. Most real processes in the boundary layer are non-Gaussian. Therefore, to estimate the systematic error of odd moments in particular, we use a non-Gaussian process with skewness and kurtosis different from 0 and 3, respectively. A simple way to construct such a process is by modifying a Gaussian process $z(t)$ with variance σ_0^2 and an exponential autocorrelation function such that

$$w(t) = z(t) + a\frac{z^2(t) - \langle z^2(t)\rangle}{\sigma_0}. \quad (19)$$

Using the Isserlis relation, it is easily seen that the skewness and kurtosis of $w(t)$ are

$$S \equiv \frac{\mu_3}{\mu_2^{3/2}} = \frac{2a(3 + 4a^2)}{(1 + 2a^2)^{3/2}},$$
$$K \equiv \frac{\mu_4}{\mu_2^2} = \frac{3(1 + 20a^2 + 20a^4)}{(1 + 2a^2)^2}. \quad (20)$$

Realistic values of a are between 0 and 0.1 for the vertical velocity w and around 0.2 for the temperature θ as seen from the right panel of Fig. 1, where values of skewness and kurtosis from the flight legs used by Lenschow and Stankov (1986) in their analysis of length scales as well as the flight legs used here, are displayed together with a parametric curve of $\{K(a), S(a)\}$ from (20). LMK derive the asymptotic systematic errors ($T \gg \mathcal{T}$) for all higher-order moments of the skewed process (19). The error of the third-order moment becomes

$$\frac{\mu_3 - \langle \mu_3(T)\rangle}{\mu_3} = 3\left[2 - \frac{1}{(1 + a^2)(3 + 4a^2)}\right]\frac{\mathcal{T}}{T}, \quad (21)$$

[1] The Isserlis relation states that, in general, the $2n$th-order moment can be reduced to a sum of $(2n-1)!!$ terms, where

$$(2n-1)!! \equiv (2n-1)\times(2n-3)\times(2n-5)\times\cdots\times 3\times 1,$$

each of which is a product of $n/2$ second-order moments.

Unauthenticated | Downloaded 02/15/25 07:08 AM UTC

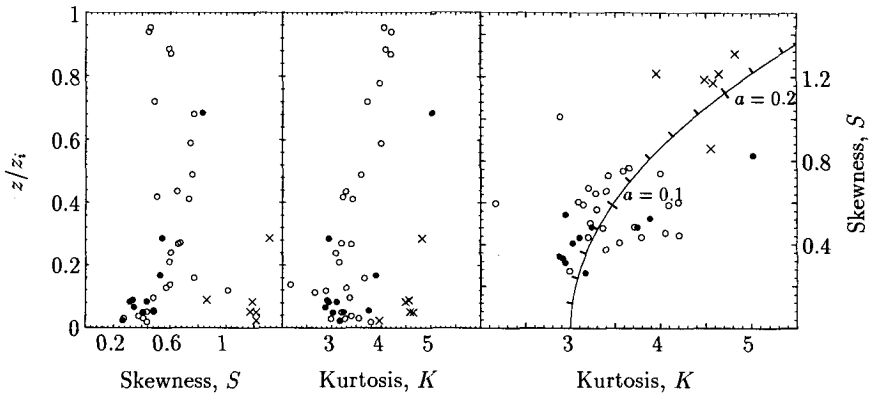

FIG. 1. Open circles are values of skewness and kurtosis of w from the flight legs used by Lenschow and Stankov (1986) in their analyses of length scales. Most of the legs are from the Air Mass Transformation Experiment and a few are from NCAR Queen Air flight legs over eastern Colorado and over the Gulf of Mexico. The flight legs varied from 42 to 170 km in length. Closed circles (w) and crosses (θ) are the values from the flight legs used in the analyses presented here, which are about 180 km in length. The right panel has the same data plotted as K versus S. The parametric curve shows the skewness and kurtosis for the process Eq. (19) as a function of the parameter a.

which is between $5\mathcal{T}/T$ and $6\mathcal{T}/T$. The systematic errors of the second- and fourth-order moments are not very different from the Gaussian results (14) and (17) (see Table 6).

b. Fluxes

It is straightforward to generalize the preceding discussion to more than one signal. It is of particular interest to extend the analysis to second-order moments of two random variables such as the vertical flux of a scalar $s(t)$. In this case $w(t)$ is the vertical velocity. Let us assume that $s(t)$ has a zero ensemble mean. Then (1)–(4) apply to $s(t)$ as well as $w(t)$. The second-order moment, that is, the flux, is defined as

$$F \equiv \langle w(t)s(t)\rangle. \tag{22}$$

Experimentally, the flux is determined as the time average

$$F(T) = \int [w(t) - w_T][s(t) - s_T]. \tag{23}$$

In general the ensemble average of $F(T)$ will be different from F. We get, in analogy to (13),

$$\langle F(T)\rangle = F - \int R_{ws}(t_2 - t_1), \tag{24}$$

where

$$R_{ws}(\tau) = \langle w(t)s(t+\tau)\rangle \tag{25}$$

is the covariance function of $w(t)$ and $s(t)$. If we define an integral timescale

$$\mathcal{T}_{ws} = \frac{1}{F}\int_0^\infty R_{ws}(\tau)d\tau \tag{26}$$

in analogy to the integral timescale for a single variable (15), then (24) can be written as

$$\frac{F - \langle F(T)\rangle}{F} \approx 2\frac{\mathcal{T}_{ws}}{T} \tag{27}$$

for $T \gg \mathcal{T}_{ws}$.

LMK discuss the difficulties in the experimental determination of $\mathcal{T}_{ws}$, which in some cases becomes negative. They therefore derive an inequality giving an upper bound on the systematic error in terms of the integral time scale of the vertical velocity $\mathcal{T}$, the integral scale of the scalar fluctuations $\mathcal{T}_s$, and the variances of these quantities, μ_2 and μ_s:

$$\frac{|F - \langle F(T)\rangle|}{(\mu_2\mu_s)^{1/2}} \leqslant 2\frac{(\mathcal{T}\mathcal{T}_s)^{1/2}}{T}. \tag{28}$$

Substituting the correlation coefficient $r_{ws} \equiv F(\mu_2\mu_s)^{-1/2}$ into (28),

$$\frac{|F - \langle F(T)\rangle|}{F} \leqslant \frac{2}{r_{ws}}\frac{(\mathcal{T}\mathcal{T}_s)^{1/2}}{T}. \tag{29}$$

LMK also derive an exact expression for the error assuming $R_{ws}(\tau)$ to be exponential, given by $R_{ws}(\tau) \equiv F\rho_{ws}(\tau) = F\exp(-|\tau|/\mathcal{T}_{ws})$, in analogy to (18):

$$\frac{F - \langle F(T)\rangle}{F} = \frac{2}{x} - \frac{2}{x^2} + \frac{2}{e^x x^2}, \tag{30}$$

where $x = T/\mathcal{T}_{ws}$.

3. Random errors

When averaging over a finite time T the time means of moments will, in general, differ from each other and from the ensemble means; that is, they are randomly

Unauthenticated | Downloaded 02/15/25 07:08 AM UTC

scattered. As in the case of systematic errors, we discuss higher moments of one quantity and fluxes separately.

a. Single time series moments

In the case of the nth-order central moment of $w(t)$, the individual realizations in an ensemble will be distributed around $\langle \mu_n(T) \rangle$ with an error variance

$$\sigma_n^2(T) = \langle [\mu_n(T) - \langle \mu_n(T) \rangle]^2 \rangle. \quad (31)$$

If we, for measuring purposes, want to determine how long we need to average in order to get a stable time-averaged value $\mu_n(T)$, that is, to get an error variance smaller than a specified value, we must find a way to estimate (31). Lenschow and Kristensen (1985) show that if the signal is a Gaussian process, for $T \gg \mathcal{T}$,

$$\sigma_2^2(T) \approx 4 \frac{\mu_2^2}{T} \int_0^\infty \rho^2(\tau) d\tau. \quad (32)$$

Similarly, taking only the first-order terms in $\mathcal{T}/T$, we get for third- and fourth-order moments

$$\sigma_3^2(T) \approx 12 \frac{\mu_2^3}{T} \int_0^\infty \rho^3(\tau) d\tau \quad (33)$$

and

$$\sigma_4^2(T) \approx 48 \frac{\mu_2^4}{T} \int_0^\infty [3\rho^2(\tau) + \rho^4(\tau)] d\tau. \quad (34)$$

Again we assume that the autocorrelation function can be represented with sufficient accuracy by the exponential (18). Therefore, we have

$$\int_0^\infty \rho^n(\tau) d\tau = \frac{\mathcal{T}}{n}, \quad (35)$$

and thus obtain the error variance estimates

$$\sigma_2^2(T) \approx 2\mu_2^2 \frac{\mathcal{T}}{T}, \quad (36)$$

$$\sigma_3^2(T) \approx 4\mu_2^3 \frac{\mathcal{T}}{T}, \quad (37)$$

and

$$\sigma_4^2(T) \approx 84\mu_2^4 \frac{\mathcal{T}}{T} \quad \text{or} \quad \sigma_4^2(T) \approx \frac{84}{9} \mu_4^2 \frac{\mathcal{T}}{T}. \quad (38)$$

LMK derive exact equations valid for all T for $\sigma_2^2(T)$, $\sigma_3^2(T)$, and $\sigma_4^2(T)$ assuming a Gaussian process and that (35) is valid. These exact error variances, normalized by μ_2 to the appropriate powers, are shown in Figs. 6, 7, and 8 (dashed lines). We note that the error variances actually go to zero as $T/\mathcal{T}$ goes to zero. Here the systematic errors correspondingly become very large.

Comparing these results with those obtained by Lumley and Panofsky (1964), and later discussed by Wyngaard (1973), we note that they state the problem of statistical uncertainty somewhat differently. We derive error variances of central moments of a time series, while they discuss powers of time series that do not have a zero time average. In other words, we extract the leading term of (31) for $T \gg \mathcal{T}$ in the form

$$\sigma_n^2(T) = \left\langle \left\{ \int [(w(t) - w_T)^n - \langle (w(t) - w_T)^n \rangle] \right\}^2 \right\rangle, \quad (39)$$

whereas Lumley and Panofsky (1964) based their asymptotic expressions on

$$\sigma_n^2(T)_{\mathrm{LP}} = \left\langle \left\{ \int [w^n(t) - \langle w^n(t) \rangle] \right\}^2 \right\rangle. \quad (40)$$

Furthermore, they use the timescale (15) as the pertinent integral scale for $w^n(t)$, irrespective of the value of n, whereas we have assumed the exponential autocorrelation function (18) and consequently obtained our integral time scale from (35).

In our notation, using our definition of the integral time scale, we find $\sigma_n^2(T)_{\mathrm{LP}} = \sigma_n^2(T)$ for Gaussian processes when n is even. This is not the case when n is odd. For example, the asymptotic error variance of the third moment, based on (40) and (35), is

$$\sigma_3^2(T)_{\mathrm{LP}} = 22\mu_3^2 \frac{\mathcal{T}}{T} = 5.5\sigma_3^2(T). \quad (41)$$

For odd moments with n larger than 3, the ratio between $\sigma_n^2(T)_{\mathrm{LP}}$ and $\sigma_n^2(T)$ decreases with n. For instance, for $n = 5$ this ratio is very close to 2, and very close to 4/3 for $n = 7$.

In contrast to the systematic errors, the random errors are significantly affected by the introduction of a realistic skewness and kurtosis using (19). These modified error variances corresponding to (36), (37), and (38) are derived in LMK and summarized in Table 6 normalized by μ_n^2, as well as in Figs. 6, 7, 8, and also Table 6 normalized by μ_2^n. The same relative error in the second-order moment requires an average twice as long for a skewed process [$a = 0.2$, in (19)] compared to a Gaussian process ($a = 0$).

b. Fluxes

In analogy to (31), we define the error variance of the flux as

$$\sigma_F^2(T) \equiv \langle [F(T) - \langle F(T) \rangle]^2 \rangle. \quad (42)$$

Inserting (23), we find

$$\sigma_F^2(T) = \int \langle f^T(t_1) f^T(t_2) \rangle, \quad (43)$$

where

$$f^T(t) = [w(t) - w_T][s(t) - s_T] - \langle [w(t) - w_T][s(t) - s_T] \rangle \quad (44)$$

Unauthenticated | Downloaded 02/15/25 07:08 AM UTC

is a time series with zero ensemble mean and defined only in the interval $-T/2 \leq t \leq T/2$. In the limit $T \to \infty$, (44) becomes a stationary time series

$$f^{\infty}(t) = w(t)s(t) - \langle w(t)w(t)\rangle. \quad (45)$$

In analogy to the derivation of the error variance of one signal, LMK show that if the variables $w(t_1)$, $s(t_2)$, $w(t_3)$, and $s(t_4)$ have a joint Gaussian probability distribution the error variance for $T \gg \mathcal{T}_f$ becomes

$$\sigma_F^2(T) \approx 2\mu_f \frac{\mathcal{T}_f}{T}, \quad (46)$$

where μ_f and $\mathcal{T}_f$ are the variance and the integral time scale, respectively, of the time series $f^{\infty}(t)$.

The relative error, which is the square root of the random error variance normalized by F^2 can be estimated from (46), after first using the Isserlis relation to expand the fourth-order moment μ_f as follows:

$$\mu_f = \mu_2\mu_s + F^2 \Rightarrow \frac{\mu_f}{F^2} = \frac{1 + r_{ws}^2}{r_{ws}^2}. \quad (47)$$

Thus, the relative error is

$$\frac{\sigma_F(T)}{|F|} = \left(\frac{2\mathcal{T}_f}{T}\right)^{1/2}\left(\frac{1 + r_{ws}^2}{r_{ws}^2}\right)^{1/2}. \quad (48)$$

In parallel to the upper limit of the systematic error (29), Lenschow and Kristensen (1985) derive an upper limit to the error variance of the flux

$$\frac{\sigma_F(T)}{|F|} \leq \frac{2}{r_{ws}}\left[\frac{\min(\mathcal{T}, \mathcal{T}_s)}{T}\right]^{1/2}, \quad (49)$$

expressed in terms of more commonly available integral time scales.

4. Disjunct sampling of fluxes

In the previous sections we have derived expressions for systematic and random errors of fluxes based on continuous sampling over finite periods with duration T. However, it is also of practical interest to experimentalists to know how many samples it is necessary to collect in the period T in order to keep the error below a specified level. In this case, we assume that the measurements are "instantaneous," that is, that the instrument response time is much smaller compared to the integral scales of w and s, and are collected at equally spaced time intervals Δ. Therefore, the error becomes a function of two time periods, T and Δ. This technique may preclude estimating spectra and integral timescales. However, the high-frequency contributions to the fluxes are retained at the possible expense of an increased systematic error and a larger statistical uncertainty.

This technique was proposed by Haugen (1978) for reducing the amount of data to be archived and to be used in computations of turbulence statistics while still maintaining acceptable error levels. Kaimal and Gaynor (1983) applied this procedure to data from BAO (Boulder Atmospheric Observatory) and called it "grab sampling." Some authors (Bendat and Piersol 1986) refer to the process as "decimation." Still another application of the technique, proposed by Cooper (1992, personal communication), is for estimating scalar fluxes using sensors with frequency responses that would not be adequate for straightforward flux measurement. With this technique, which Cooper calls "intermittent sampling," the samples are grabbed quickly in a time interval that determines the temporal resolution of the measurement; the scalar quantity is then measured over a longer period, compatible with the time response of the sensor. We suggest the term "disjunct sampling" for this process, since it conveys the interpretation of separation between data points, while decimation means literally taking every tenth sample and intermittency already has a quite separate meaning in the context of turbulent flows.

We illustrate these considerations, with only small modifications in the derivation from the case with continuous sampling, by considering measurements of the flux of a scalar $s(t)$ at equidistant time intervals Δ over a total record length T, although the technique is applicable to other turbulence statistics as well. The number of sampled points is

$$N = \frac{T}{\Delta}. \quad (50)$$

The time averages are now

$$w_{T,\Delta} = \frac{1}{N}\sum_{l=0}^{N-1} w(l\Delta), \quad (51)$$

$$s_{T,\Delta} = \frac{1}{N}\sum_{l=0}^{N-1} s(l\Delta). \quad (52)$$

The time average of the flux is, in analogy to (23),

$$F(T, \Delta) = \frac{1}{N}\sum_{l=0}^{N-1}[w(l\Delta) - w_{T,\Delta}][s(l\Delta) - s_{T,\Delta}]. \quad (53)$$

The ensemble average of $F(T, \Delta)$ now becomes

$$\langle F(T, \Delta)\rangle = F - \frac{1}{N}\sum_{l_1=0}^{N-1}\frac{1}{N}\sum_{l_2=0}^{N-1}\langle w(l_1\Delta)s(l_2\Delta)\rangle. \quad (54)$$

If we assume, as in the preceding sections, that the covariance function ρ_{ws} is exponential, then it is straightforward to evaluate (54) exactly for all values of $N = T/\Delta \gg 1$. We get

$$\frac{F - \langle F(T, \Delta)\rangle}{F}\frac{T}{\mathcal{T}_{ws}} = \frac{\Delta}{\mathcal{T}_{ws}}\left\{\coth\left(\frac{\Delta}{2\mathcal{T}_{ws}}\right) - \frac{(\Delta/\mathcal{T}_{ws})(\mathcal{T}_{ws}/T)[1 - \exp(-T/\mathcal{T}_{ws})]}{2\sinh^2(\Delta/2\mathcal{T}_{ws})}\right\}. \quad (55)$$

Unauthenticated | Downloaded 02/15/25 07:08 AM UTC

The two asymptotes of the relative systematic error can be written, for $T \gg \mathcal{T}_{ws}$, as

$$\frac{F - \langle F(T, \Delta)\rangle}{F}\frac{T}{\mathcal{T}_{ws}} = \begin{cases} 2, & \Delta \ll \mathcal{T}_{ws} \\ \dfrac{\Delta}{\mathcal{T}_{ws}}, & \Delta \gg \mathcal{T}_{ws} \end{cases}. \quad (56)$$

This result does not depend on the assumption of an exponential covariance function.

For disjunct sampling, the error variance becomes

$$\sigma_F^2(T, \Delta) = \frac{1}{N}\sum_{l_1=0}^{N-1}\frac{1}{N}\sum_{l_2=0}^{N-1}\langle f^\infty(l_1\Delta)f^\infty(l_2\Delta)\rangle + O\left(\frac{1}{N^2}\right), \quad (57)$$

which to first order in $\Delta/T = 1/N \ll 1$ becomes, for an exponential covariance function,

$$\frac{\sigma_F^2(T, \Delta)}{\mu_f}\frac{T}{\mathcal{T}_f} = \frac{\Delta}{\mathcal{T}_f}\coth\left(\frac{\Delta}{2\mathcal{T}_f}\right) \quad (58)$$

(see LMK for a derivation). Normalizing the error variance by $\mu_f\mathcal{T}_f/T$, the asymptotes can be written, for $T \gg \mathcal{T}_f$, as

$$\frac{\sigma_F^2(T, \Delta)}{\mu_f}\frac{T}{\mathcal{T}_f} = \begin{cases} 2, & \Delta \ll \mathcal{T}_f \\ \dfrac{\Delta}{\mathcal{T}_f}, & \Delta \gg \mathcal{T}_f \end{cases}, \quad (59)$$

independent of the assumption of an exponential covariance function.

Equation (58) was also obtained by Cooper (1992, personal communication). For $T \gg \mathcal{T}_{ws}$, the second term in (55) in negligible, so that the systematic and random errors have a similar dependence on the ratio of Δ and the appropriate integral scale.

5. Experimental validation

Here we compare the theoretical expressions derived in the previous sections with moment errors calculated from actual time series. We use vertical air velocity w and temperature θ measured by the National Center for Atmospheric Research (NCAR) Electra aircraft during two field campaigns: 1) a set of ten 30-min flight legs over the East China Sea during wintertime cold-air outbreaks over a relatively warm ocean surface, and 2) one 30-min leg over land in the daytime convective boundary layer. The first campaign took place in February 1975 as part of the Air Mass Transformation Experiment (AMTEX), which is described by Lenschow and Agee (1976). The second campaign, Electra Radome Experiment (ELDOME), was carried out in May 1988 over the sand-hill country of western Nebraska, where the rolling hills (stabilized sand dunes) extend to a height of up to 80 m. We include this leg of comparison with the over-water flight legs from AMTEX. A summary of flight parameters is given in Table 1. Prior to the analysis, a linear trend was removed from all the time series to eliminate contributions from large-scale variability and instrument drift.

For each of the flight legs we calculated the three moments μ_2, μ_3, and μ_4, the corresponding values of the skewness S and the kurtosis K, and the integral scale $\mathcal{T}$ for the vertical velocity w. The integral scale was obtained from the spectrum of w by a least-squares fit to the function

$$\Phi_{ww}(\omega) = \frac{\mathcal{T}\mu_2}{\pi}\frac{1}{1 + \omega^2\mathcal{T}^2}, \quad (60)$$

which is the Fourier transform of the autocorrelation function (18). The results of these calculations are shown in Table 2. We note that most of the integral time scales are about 1 s or less. However, two of the time series (AMTEX03 and AMTEX07) have time scales around 2 s. The values of z/z_i for these flight legs were 0.7 and 0.3, that is, cruising heights well into the boundary layer.

The temperature signals $\theta(t)$ were generally of lower quality than the velocity data, and as shown in Table 3, not all the temperature time series could be used because of noise and other instrument problems. In the remaining temperature time series the mesoscale structures were removed by a symmetric Gaussian high-pass filter with a time constant that was 100 times the integral timescale $\mathcal{T}$ of the concurrent w time series. This removes temperature fluctuations at scales larger than about 10–20 times the depth of the boundary layer z_i. After this filtering, the selected temperature time series were analyzed in the same way as w to obtain moments and the integral timescales $\mathcal{T}_s$. The results are shown in Table 3. The values of $\mathcal{T}_s$ are generally about 50% larger than for $\mathcal{T}$, in contrast to Lenschow and Stankov (1986), who obtained values of $\mathcal{T}_s$ about six times larger than $\mathcal{T}$. This is likely due to their use

TABLE 1. Time, true airspeed, height above the surface z, and inversion height z_i for the airplane flight legs used in the data analysis.

Name	Date	Period (LST)	Airspeed (m s^{-1})	z (m)	z_i (m)
AMTEX01	15 February 1975	1130–1200	97.3	100	1200
AMTEX02	16 February 1975	1136–1206	104.0	95	1430
AMTEX03	16 February 1975	1611–1641	108.0	980	1430
AMTEX04	18 February 1975	1102–1132	103.7	90	1010
AMTEX05	18 February 1975	1430–1500	103.5	85	1010
AMTEX06	19 February 1975	1047–1117	101.8	95	1842
AMTEX07	21 February 1975	1202–1232	100.9	315	1100
AMTEX08	22 February 1975	1204–1234	99.2	95	1900
AMTEX09	28 February 1975	1242–1312	105.4	95	1700
AMTEX10	28 February 1975	1328–1358	106.4	285	1700
ELDOME	12 May 1988	1412–1442	101.0	70*	2950

* 30–100 m.

Unauthenticated | Downloaded 02/15/25 07:08 AM UTC

TABLE 2. Moments and integral scales of w for the analyzed flight legs.

Name	μ_2 $(\text{m s}^{-1})^2$	μ_3 $(\text{m s}^{-1})^3$	μ_4 $(\text{m s}^{-1})^4$	S	K	$\mathcal{T}$ (s)
AMTEX01	1.060	0.342	3.303	0.313	2.938	1.045
AMTEX02	1.105	0.398	3.507	0.343	2.872	0.789
AMTEX03	1.122	0.983	6.326	0.827	5.022	2.504
AMTEX04	0.420	0.091	0.513	0.334	2.909	0.754
AMTEX05	0.576	0.190	1.030	0.434	3.100	0.681
AMTEX06	1.257	0.682	5.116	0.484	3.238	1.200
AMTEX07	1.963	1.496	11.339	0.544	2.943	1.879
AMTEX08	1.110	0.475	3.724	0.407	3.025	0.681
AMTEX09	0.213	0.047	0.170	0.483	3.747	0.583
AMTEX10	0.187	0.042	0.136	0.526	3.886	0.737
ELDOME	0.885	0.220	2.479	0.264	3.165	1.038

of unfiltered temperature time series (although they used legs mostly of from 50 to 100 km length) and their use of the autocorrelation function only up to the first zero crossing for computing the integral scale.

We then computed the cospectrum of temperature and velocity and the power spectrum of the product time series (45) to obtain, by fitting to a spectrum of the type (60), the integral timescales $\mathcal{T}_{ws}$ and $\mathcal{T}_f$. These are presented in Table 4, together with the estimated values of the flux F and the variance μ_f of the product.

Figure 2 shows an example of the analysis procedure. The time series are divided into subseries of length T from which the moments $\mu_2(T)$, $\mu_3(T)$, and $\mu_4(T)$ are calculated. Even though T is of the order of 25 time scales, the means (indicated by broad horizontal lines) are not equal to the mean of the entire time series shown by the thin horizontal line. This has the consequence that second- and higher-order moments are slightly underestimated as predicted in section 2.

Assuming the entire time series to be stationary, the averages of the estimates of the moments represent $\langle \mu_n(T) \rangle$, which are shown in Figs. 3, 4, and 5 as functions of $T/\mathcal{T}$. The means of the moments estimated from a time series of length T are normalized by μ_n determined from the entire time series in order to compare with the theoretical expressions. For the second moment we compare to the exact expression [LMK their Eq. (A1)], which is valid both for a Gaussian and the skewed process (19) provided that the autocorrelation is exponential. The experimental systematic errors of the third moment are compared to [LMK their Eq. (A3)], which is derived from the very skewed process [$a \to \infty$ in (19)], and errors of the fourth moment are compared to [LMK their Eq. (A2)], derived from the Gaussian process. The systematic error of the second moment is well predicted. The estimates of the systematic error of the third moment have more scatter and the error of the fourth moment is generally less than predicted. The error of the temperature moments tends to be smaller than for the vertical velocity moments, which might be due to the filtering. The asymptotic expressions differ significantly from the exact ones only at very small averaging times.

The variances of the estimates of the nth moment normalized by μ_2^n versus averaging time divided by the time scale are shown in Figs. 6, 7, and 8. Generally, the error variance estimates for a Gaussian process in section 3 are lower limits for the error variance of the moment estimates for the atmospheric signals. The estimates are improved when we use the results from the skewed process (19) from Table 6. This can be seen most clearly in Fig. 7 where the temperature, which generally has larger skewness than the velocity signal, has larger error variance. From Tables 2 and 3 and Fig. 1, it can be seen that $a \approx 0.2$ for the temperature signals and that a is between zero and 0.1 for the velocity. The velocity signal from AMTEX03 has an ex-

TABLE 3. Moments and integral scales of θ for the analyzed flight legs.

Name	μ_2 (K^2)	μ_3 (K^3)	μ_4 (K^4)	S	K	$\mathcal{T}_s$ (s)
AMTEX01	0.0297	0.00610	0.00397	1.188	4.490	1.249
AMTEX04	0.00547	0.000348	0.000137	0.860	4.558	1.354
AMTEX06	0.0479	0.0123	0.0105	1.173	4.583	1.456
AMTEX07	0.0225	0.00441	0.00294	1.311	4.826	2.266
AMTEX08	0.0398	0.00964	0.00737	1.215	4.649	1.034
ELDOME	0.0470	0.0124	0.0110	1.216	3.962	1.528

TABLE 4. Fluxes, variances of the fluxes, and flux integral scales of θ.

Name	F (m s^{-1} K)	μ_f $(\text{m s}^{-1}\ \text{K})^2$	$\mathcal{T}_{ws}$ (s)	$\mathcal{T}_f$ (s)
AMTEX01	0.1073	0.0467	1.277	0.419
AMTEX04	0.0263	0.00370	0.982	0.306
AMTEX06	0.1534	0.1067	1.563	0.488
AMTEX07	0.1118	0.0891	1.898	0.894
AMTEX08	0.1290	0.0719	0.937	0.326
ELDOME	0.0896	0.06055	1.597	0.356

Unauthenticated | Downloaded 02/15/25 07:08 AM UTC

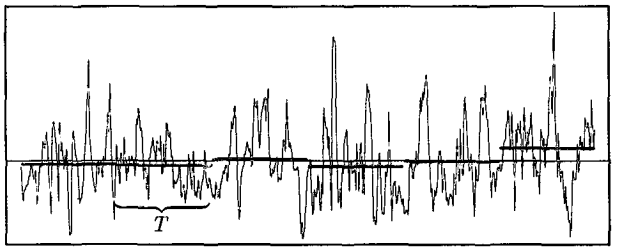

FIG. 2. Subdivision of a time series in "realizations" of length T.

ceptionally large skewness and kurtosis and therefore has large error variances (see the uppermost thin solid lines in Figs. 7 and 8). The spread of the curves in Fig. 6 for $T/\mathcal{T} \approx 1000$ is partly due to poor statistics. Only three estimates of μ_n were made here for each half-hour time series giving an uncertain determination of $\sigma_n^2(T)$. We do not know why the error variance of one run, AMTEX07, drops significantly below the Gaussian estimate for both $n = 2$ and $n = 4$.

To test the theory of random and systematic errors of flux measurements both the scalar (temperature) and the vertical velocity signal were subdivided into shorter pieces of length T as shown in Fig. 2. The averages w_T and s_T were subtracted and the flux was estimated according to (23). For the disjunctly sampled flux, (53) was used to estimate the flux, and in order to use all the information in the data and not only data points separated by Δ, we permitted the intervals of length T, used to estimate $F(T, \Delta)$, to be overlapping. This improved the statistics of the estimates of $\langle F(T, \Delta)\rangle$ and $\sigma_F^2(T, \Delta)$.

As seen from Fig. 9 the theory predicts the systematic errors of the flux estimates well. For the random error variance, however, there is a large spread around the theory as shown in Figs. 10 and 11. Among the reasons

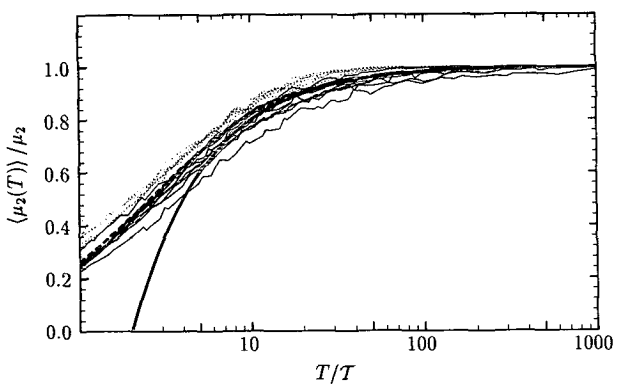

FIG. 3. Normalized second-order moment of vertical velocity (solid lines) and temperature (dotted lines) versus observation time T divided by the timescale $\mathcal{T}$ or $\mathcal{T}_s$ (see Tables 2 and 3). The broad solid line is the asymptotic expression Eq. (14); the dashed line almost obscured by the data curves is the exact expression valid for all $T/\mathcal{T}$ assuming exponential autocorrelation [LMK their Eq. (A1)].

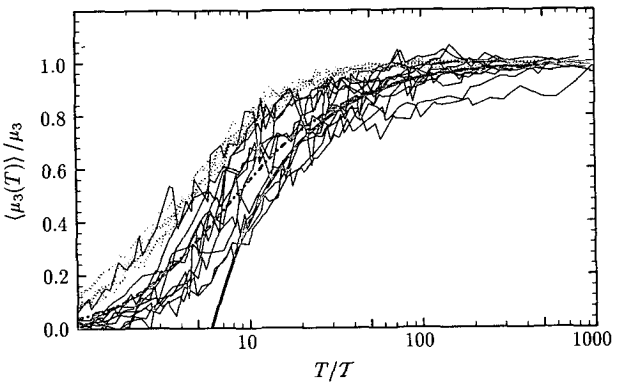

FIG. 4. Normalized third-order moments. See caption of Fig. 3. The solid line is the asymptotic expression, $1 - 6T/\mathcal{T}$ [from LMK Eq. (B37) with $a = \infty$ in Eq. (19)], and the dot-dash the exact, [LMK their Eq. (A3)], also with $a = \infty$.

for this spread are poor statistics for large T and nonstationarities in the product time series $s(t)w(t)$, which were not obvious from a visual inspection of the time series. We conclude that (46) is slightly superior to (49) as an estimate of the error variance. The data analysis shown in Fig. 12 supports the asymptotic expression (58) for the error variance of disjunctly sampled fluxes, although the data points are somewhat scattered.

6. Discussion and conclusions

Several previous evaluations of statistical errors of moments and fluxes have been carried out subsequent to the analysis of Lumley and Panofsky (1964). For example, Sreenivasan et al. (1978) investigated statistical errors of moments and fluxes using wind velocity, temperature, and humidity measurements at a height of 5 m above MSL over Bass Strait off the Gippsland coast of Victoria, Australia. The conditions were slightly unstable with a Monin–Obukhov length of

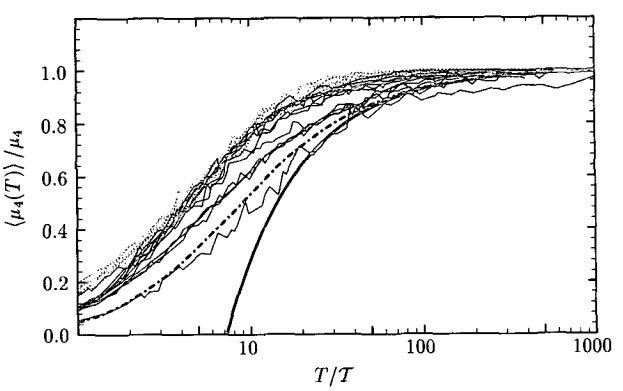

FIG. 5. Normalized fourth-order moments. See caption of Fig. 3. The solid line is the asymptotic expression Eq. (17), and the dot-dash the exact for the Gaussian process [LMK their Eq. (A2)].

Unauthenticated | Downloaded 02/15/25 07:08 AM UTC

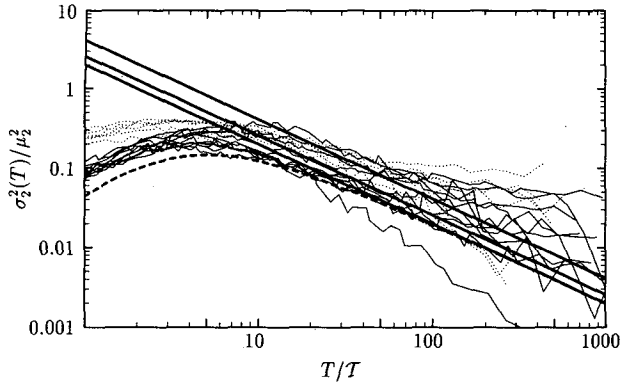

FIG. 6. Normalized random error variance of the second-order moment of vertical velocity (solid lines) and temperature (dotted lines) versus observation time T divided by the timescale $\mathcal{T}$ or $\mathcal{T}_s$ (see Tables 2 and 4). The three straight lines are the asymptotic expression from Table 6 for $a = 0$, $a = 0.1$, and $a = 0.2$ with $a = 0$ as the lower, and $a = 0.2$ as the upper line. The dashed line is the exact expression for the error variance for the Gaussian process [LMK their Eq. (A5)].

about −100 m. Our data are from the convective boundary layer and consequently we observe somewhat higher values of skewness S and kurtosis K. In Table 5 we compare their relative error variances of second and fourth moments of w ($a = 0.1$) and θ ($a = 0.2$) with ours. The normalized relative error variances for Gaussian processes with exponential autocorrelation functions are 2 and $28/3 \approx 9.3$ for second- and fourth-order moments, respectively. We notice that for both orders the results of Sreenivasan et al. (1978) are indeed not far from the predictions for Gaussian variables, as they pointed out. However, our results show that the error variances, in particular that for the fourth-order moment, vary significantly with deviations from a Gaussian process.

In view of the general agreement between theory and experiment, we now feel confident in addressing

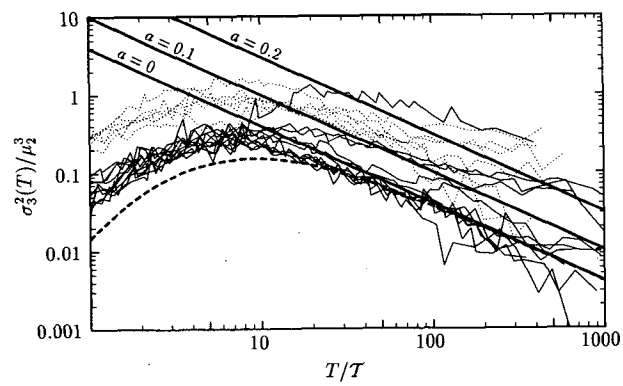

FIG. 7. Normalized error variance of the third-order moment. See caption of Fig. 6 and Table 6. The dashed line is the exact expression for the Gaussian process [LMK their Eq. (A6)].

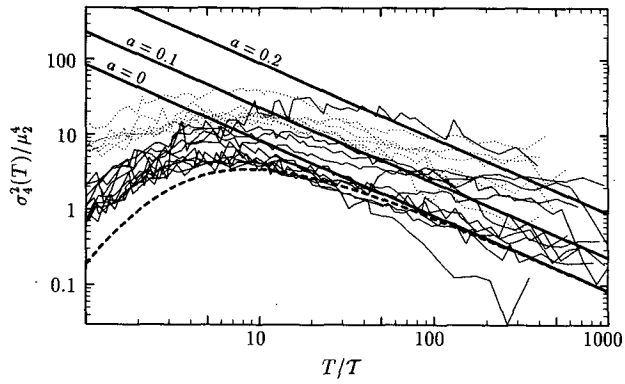

FIG. 8. Normalized error variance of the fourth-order moment. See caption of Fig. 6 and Table 6. The dashed line is the exact expression for the Gaussian process [LMK their Eq. (A7)].

the question of how long is "long enough" when measuring fluxes and other turbulent statistics. We first consider continuous sampling of higher moments and fluxes. Table 6 summarizes our results for both systematic and random errors of continuously sampled moments. Applying (28) and (49), and assuming on basis of the data in Tables 2 and 3 that $\mathcal{T}_s \approx \mathcal{T}$, we arrive at the general result for the ratios of the errors

$$\frac{\sigma_n(T)}{\mu_n - \langle \mu_n(T) \rangle} \approx \frac{\sigma_F(T)}{|F - \langle F(T) \rangle|} \approx A\left(\frac{T}{\mathcal{T}}\right)^{1/2}, \quad (61)$$

where A is a dimensionless constant of order unity for the one-variable moments. (For fluxes, A is not necessarily close to unity.) Equation (61) and Table 6 tell us that for $T \gg \mathcal{T}$, the systematic error becomes small and the random error is much greater than the systematic error, so that we can generally disregard the systematic error.

As an example, we estimate how long an airplane flight leg is required to estimate μ_4 with an error of

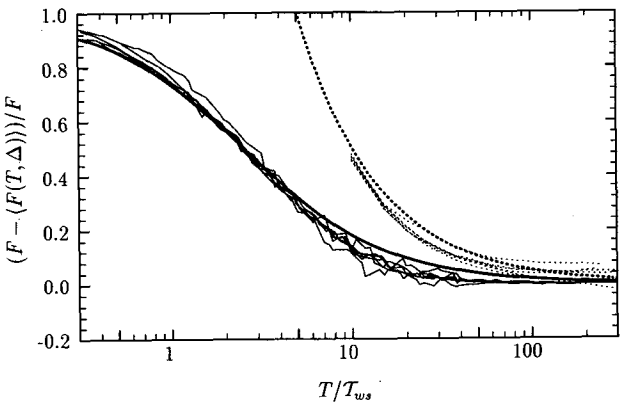

FIG. 9. Systematic error of continuously sampled fluxes (thin solid lines) and disjunctly sampled fluxes (thin dotted lines) with $\Delta/\mathcal{T}_{ws} = 5$. The lower broad curve is Eq. (30) while the upper dotted broad curve is Eq. (55).

Unauthenticated | Downloaded 02/15/25 07:08 AM UTC

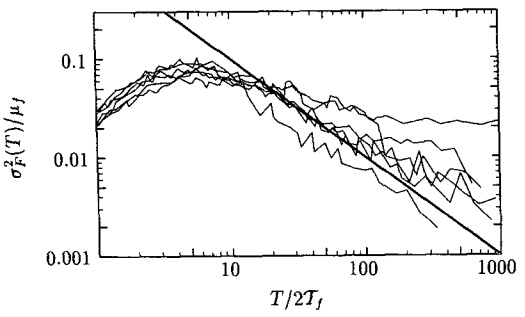

FIG. 10. Normalized random error variance of the vertical flux of temperature. The broad line is the asymptotic expression Eq. (46).

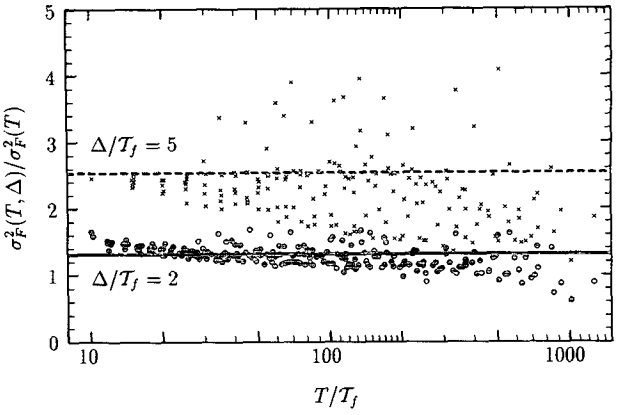

FIG. 12. Normalized random error variance $\sigma_F^2(T, \Delta)/\sigma_F^2(T)$ of disjunctly sampled fluxes of temperature. Dots have $\Delta/\mathcal{T}_f = 2$ while the crosses have $\Delta/\mathcal{T}_f = 5$. The horizontal lines are the asymptotic expression Eq. (58) valid for $N = T/\Delta \gg 1$ normalized by Eq. (46).

10%. Neglecting the observation that the measured kurtosis in the boundary layer is larger than for a Gaussian process, we estimate that $\sigma_4(T)/\mu_4 \approx 0.10 \approx 3(\mathcal{L}/L)^{1/2}$, where we have now transformed from the time to the space domain, and use L as the averaging length and $\mathcal{L}$ as the integral length scale. Thus $L \approx 900\mathcal{L}$ or, since $\mathcal{L} \approx 100$ m, $L \approx 90$ km. With these values of L and $\mathcal{L}$ the systematic error becomes approximately 0.4%. If we assume the time series to be as skewed as the temperature measurements analyzed here ($a \approx 0.2$), the flight leg would have to be $L \approx 40\mathcal{L}/(0.10)^2 \approx 400$ km.

The approach here complements that of Lenschow and Stankov (1986), who used the formulation of Lumley and Panofsky (1964) and estimated integral scales of the second moments from aircraft observations. They did not consider systematic errors nor the effects of non-Gaussianity on the errors. A situation where the systematic error becomes relevant is when trying to evaluate a scalar flux from an area of limited extent with aircraft measurements. From Lenschow and Stankov (1986) the integral length scales for w and a scalar s are $\mathcal{L} \approx 0.24 z_i(z/z_i)^{1/2}$ and $\mathcal{L}_s \approx 1.49 z_i(z/z_i)^{1/2}$, respectively, and the value they used for the correlation coefficient in the lower part of the mixed layer is

$$r_{ws} \equiv \frac{F_0}{(\mu_2\mu_s)^{1/2}} \approx 0.56\,, \tag{62}$$

where F_0 is the surface flux. [We know of no similar general formulation in the literature for $\mathcal{L}_{ws}$, so we cannot use (27).] Therefore, from (29) the systematic error, expressed here as a function of the length L of the particular flight segment, is given by

$$\left|\frac{F - \langle F(L)\rangle}{F}\right| \leqslant \frac{1.2 z_i(z/z_i)^{1/2}}{|r_{ws}|\,L}\,. \tag{63}$$

Thus, the systematic error in the lower part of the mixed layer normalized by the surface flux is

$$\frac{|F_0 - \langle F_0(L)\rangle|}{F_0} \leqslant \frac{2.2 z_i(z/z_i)^{1/2}}{L}\,. \tag{64}$$

As an example, if $z_i = 1000$ m, $L = 4000$ m, and $z = 100$ m, the systematic error is less than or equal to 17%.

Using the integral length scale for the flux in the mixed layer given by Lenschow and Stankov (1986), $\mathcal{L}_f \approx 0.16 z_i(z/z_i)^{1/3}$, in (48) and (62) we get

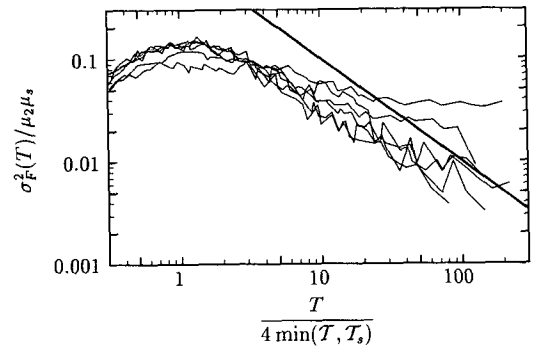

FIG. 11. Normalized random error variance of the vertical flux of temperature. The broad line is the square of the asymptotic expression Eq. (49).

TABLE 5. Comparison between the results of Sreenivasan et al. (1978) (SCA) and the present analysis (LMK) for random errors of second and fourth order.

	w		θ	
	SCA	LMK	SCA	LMK
S	0.02	~0.4	0.39	~1.0
K	3.16	~3.5	3.05	~4.5
$\frac{T}{\mathcal{T}}\frac{\sigma_2^2(T)}{\mu_2^2}$	2.2	2.6	2.9	4.0
$\frac{T}{\mathcal{T}}\frac{\sigma_4^2(T)}{\mu_4^2}$	10.5	19.0	10.9	40.0

Unauthenticated | Downloaded 02/15/25 07:08 AM UTC

TABLE 6. Systematic and random errors of second-, third- and fourth-order moments. The Gaussian process has $a = 0$, while $a = 0.1$ and $a = 0.2$ [in Eq. (19)] correspond to skewnesses typical for the vertical velocities and temperatures analyzed here. The random errors are normalized in two different ways.

	$\frac{\mu_2 - \langle\mu_2(T)\rangle}{\mu_2}\frac{T}{\mathcal{T}}$	$\frac{\mu_3 - \langle\mu_3(T)\rangle}{\mu_3}\frac{T}{\mathcal{T}}$	$\frac{\mu_4 - \langle\mu_4(T)\rangle}{\mu_4}\frac{T}{\mathcal{T}}$
$a = 0$	2	—	4
$a = 0.1$	2	5.02	4.3
$a = 0.2$	2	5.09	4.8
	$\frac{\sigma_2^2(T)}{\mu_2^2}\frac{T}{\mathcal{T}}$	$\frac{\sigma_3^2(T)}{\mu_3^2}\frac{T}{\mathcal{T}}$	$\frac{\sigma_4^2(T)}{\mu_4^2}\frac{T}{\mathcal{T}}$
$a = 0$	2	—	9.3
$a = 0.1$	2.6	29	19
$a = 0.2$	4.1	24	40
	$\frac{\sigma_2^2(T)}{\mu_2^2}\frac{T}{\mathcal{T}}$	$\frac{\sigma_3^2(T)}{\mu_2^3}\frac{T}{\mathcal{T}}$	$\frac{\sigma_4^2(T)}{\mu_2^4}\frac{T}{\mathcal{T}}$
$a = 0$	2	4	84
$a = 0.1$	2.57	9.97	231
$a = 0.2$	4.12	30.6	897

$$\frac{\sigma_F(L)}{|F|} = 1.16\left(\frac{z}{z_i}\right)^{1/6}\left(\frac{z_i}{L}\right)^{1/2}. \tag{65}$$

The result for the above example is 39%.

Substituting (62) and the expression for $\mathcal{L}$ into the alternative expression (49) we have, since $\mathcal{L} \leqslant \mathcal{L}_s$,

$$\frac{\sigma_F(L)}{|F|} \leqslant 1.75\left(\frac{z}{z_i}\right)^{1/4}\left(\frac{z_i}{L}\right)^{1/2}. \tag{66}$$

The result for the above example is less than or equal to 49%.

We see that the random error is more than twice the systematic error. To reduce the random error to less than 10%, we would have to fly over the same 4-km section 16 times. This would not, of course, reduce the systematic error. If we extend the flight segment to 20 km, however, the systematic error is reduced to less than or equal to 4%, while the random error is approximately 18%. Thus, the systematic error rapidly becomes negligible while the random error may still be significant. This means that a running integral of the cospectrum from high frequency to low frequency, as utilized by, for example, Friehe et al. (1988), may approach a particular estimate of the flux, but that particular value will still have random scatter associated with it that will require further averaging to reduce.

In the above example, we have estimated the errors in a measured flux by normalizing by the flux at that level. This is often not as appropriate as the surface flux since the surface flux is used as a scaling parameter in both the surface layer and the mixed layer. In the lowest 10% of the boundary layer the flux is often assumed to be equal to the surface flux. In other cases, it may be preferable to normalize by the flux at the measurement height, since the errors would be the relative errors at that particular level. The disadvantage of using the flux at the measurement height is that in some cases (e.g., the buoyancy flux at some level in the upper part of the mixed layer) the flux goes to zero so that the relative error becomes large for any reasonable measurement length.

In the case of stress or momentum flux measurement, Lenschow and Stankov (1986) point out that in the mixed layer generally considerably longer averaging lengths are required than for scalar fluxes to achieve the same accuracy. This follows from having a correlation coefficient that is smaller than for scalars, which more than compensates for the momentum flux having an integral scale about 75% that of scalars. Consideration of the momentum flux is somewhat more complicated than scalar fluxes since in the mixed layer the correlation coefficient depends on both z/z_i and on the ratio of the Monin–Obukhov length L_{MO} to z_i. From the results of Lenschow et al. (1980), we obtain for the correlation coefficient of the wind component along the direction of flow in the lower part of the mixed layer, where the momentum and temperature fluxes are assumed to have their surface values:

$$r_{wu} \approx 0.74\left(\frac{-L_{MO}}{z_i}\right)^{2/3}\left(\frac{z}{z_i}\right)^{-1/3}. \tag{67}$$

This means that in most cases $r_{wu} < 0.25$ and that typically the averaging lengths for momentum flux will be several times that for scalar fluxes for the same accuracy.

The results in this paper can also be presented from the perspective of spectra and cospectra by noting that the integral timescale for an exponential autocorrelation (or correlation) function is related to the frequency of the peak in the corresponding spectrum (or cospectrum) (60) multiplied by frequency. The relation is $\omega_m = \mathcal{T}^{-1}$. The corresponding relationship between the integral length scale and the wavelength of the spectral maximum is $\lambda = 2\pi\mathcal{L}$.

We have used mixed-layer scaling for the examples here, but similar formulations can be obtained and applied to the surface layer. From the flux cospectrum presented by Wesely et al. (1989), the integral length scale for scalar fluxes in the surface layer is $\mathcal{L}_{ws}/z \approx 1.6$, while from the spectra presented by Kaimal et al. (1972), $\mathcal{L}/z$ ranges from approximately 0.3 to 1.0, depending on stability.

Both theory and data show that disjunct sampling of fluxes does not appreciably increase the systematic error and the error variance by much until the time between samples Δ becomes several times the appropriate integral scale. For example, (58) shows that for the same total averaging time T, σ_F^2 is about 8% larger than for continuous sampling when $\Delta = \mathcal{T}_f$, increasing to 31% and 250% when $\Delta/\mathcal{T}_f$ is increased to 2 and 5,

Unauthenticated | Downloaded 02/15/25 07:08 AM UTC

respectively. The same is true for the systematic error using $\mathcal{T}_{ws}$ for the integral scale with the condition that $T \gg \mathcal{T}_{ws}$. From this point of view it seems that it is possible to use rather slow sensors with a temporal resolution of several seconds for flux measurements in the mixed layer without appreciable loss of statistical significance if the sample is grabbed quickly.

Acknowledgments. We acknowledge the contributions of Art Isbell, Mike Dipurna, John DeSanto, and Michelle Querijero, who developed programs and carried out calculations of moments from aircraft data. Peter Kirkegaard provided helpful clarification of the use of the Isserlis relation. We also acknowledge the contributions of the NCAR Research Aviation Facility in conducting the Electra research flights and processing the aircraft datasets. Helpful comments on the manuscript were received from Tom Horst and Steve Oncley. We are particularly grateful to one of the referees for several helpful comments including suggesting the modified Gaussian process (19).

REFERENCES

Bendat, J. S., and A. G. Piersol, 1986: *Random Data, Analysis and Measurement Procedures.* 2d ed. John Wiley & Sons, 566 pp.

Betts, A. K., R. L. Desjardins, J. I. MacPherson, and R. D. Kelly, 1990: Boundary-layer heat and moisture budgets from FIFE. *Bound.-Layer Meteor.*, **50**, 109–137.

Friehe, C. A., E. R. Williams, and R. L. Grossman, 1988: An intercomparison of two aircraft gust probe systems. *Symp. on Lower Tropospheric Profiling,* Boulder, CO, Amer. Meteor. Soc., 235F–236F.

Grossman, R. L., 1992: Sampling errors in the vertical fluxes of potential temperature and moisture measured by aircraft during FIFE. *J. Geophys. Res.*, **97**(D17), 18 439–18 443.

Haugen, D. A., 1978: Effects of sampling rates and averaging periods on meteorological measurements. *Proc. Fourth Symp. on Meteorological Observations and Instrumentation,* Denver, CO, Amer. Meteor. Soc., 15–18.

Kaimal, J. C., and J. E. Gaynor, 1983: The Boulder Atmospheric Observatory. *J. Climate Appl. Meteor.*, **22**, 863–880.

——, J. C. Wyngaard, Y. Izumi, and O. R. Coté, 1972: Spectral characteristics of surface-layer turbulence. *Quart. J. Roy. Meteor. Soc.*, **98**, 563–589.

Kelly, R. D., E. A. Smith, and J. I. MacPherson, 1992: A comparison of surface sensible and latent heat fluxes from aircraft and surface measurements in FIFE 1987. *J. Geophys. Res.*, **97**(D17), 18 445–18 453.

Koopmans, L. H., 1974: *The Spectral Analysis of Time Series.* Academic Press, 368 pp.

LeMone, M. A., 1990: Some observations of vertical-velocity skewness in the convective planetary boundary layer. *J. Atmos. Sci.*, **47**, 1163–1169.

Lenschow, D. H., and E. M. Agee, 1976: Preliminary results from the Air Mass Transformation Experiment (AMTEX). *Bull. Amer. Meteor. Soc.*, **57**, 1346–1355.

——, and L. Kristensen, 1985: Uncorrelated noise in turbulence measurements. *J. Atmos. Oceanic Technol.*, **2**, 68–81.

——, and B. B. Stankov, 1986: Length scales in the convective boundary layer. *J. Atmos. Sci.*, **43**, 1198–1209.

——, and B. B. Hicks, 1989: *Global Tropospheric Chemistry: Chemical Fluxes in the Global Atmosphere.* National Center for Atmospheric Research, 107 pp.

——, J. C. Wyngaard, and W. T. Pennell, 1980: Mean-field and second-moment budgets in a baroclinic, convective boundary layer. *J. Atmos. Sci.*, **37**, 1313–1326.

——, J. Mann, and L. Kristensen, 1993: How long is long enough when measuring fluxes and other turbulence statistics? NCAR/TN-389 + STR, 53 pp. [Available from NCAR, P.O. Box 3000, Boulder, CO 80307.]

Lumley, J. L., and H. A. Panofsky, 1964: *The Structure of Atmospheric Turbulence.* John Wiley & Sons, 239 pp.

Mason, P. J., 1989: Large eddy simulation of the convective atmospheric boundary layer. *J. Atmos. Sci.*, **46**, 1492–1516.

Moeng, C.-H., and R. Rotunno, 1990: Vertical-velocity skewness in the buoyancy-driven boundary layer. *J. Atmos. Sci.*, **47**, 1149–1162.

Schmidt, H., and U. Schumann, 1989: Coherent structure of the convective boundary layer derived from large-eddy simulations. *J. Fluid Mech.*, **200**, 511–562.

Sreenivasan, K. R., A. J. Chambers, and R. A. Antonia, 1978: Accuracy of moments of velocity and scalar fluctuations in the atmospheric surface layer. *Bound.-Layer Meteor.*, **14**, 341–359.

Wesely, M. L., D. H. Lenschow, and O. T. Denmead, 1989: Flux measurement techniques. *Global Tropospheric Chemistry: Chemical Fluxes in the Global Atmosphere,* D. H. Lenschow and B. B. Hicks, Eds., NCAR, 31–46.

Wyngaard, J. C., 1973: On surface-layer turbulence. *Workshop on Micrometeorology,* D. A. Haugen, Ed., Amer. Meteor. Soc., 101–149.

Unauthenticated | Downloaded 02/15/25 07:08 AM UTC